Chemistry–A European Journal
Research Article
doi.org/10.1002/chem.202402297
Chemistry Europe
European Chemical Societies Publishing
www.chemeurj.org

On-Surface Stepwise Double Dehydrogenation for the Formation of a *para*-Quinodimethane-Containing Undecacene Isomer

Suchetana Sarkar,[a] Berta Álvarez,[b] Kwan Ho Au-Yeung,[a, f] Agustín Cobas,[c] Roberto Robles,[d] Nicolás Lorente,[e] Diego Peña,*[b] Dolores Pérez,*[b, c] and Francesca Moresco*[a]

The on-surface synthesis of an isomer of undecacene, bearing two four-membered rings and two *para*-quinodimethane moieties, starting from a tetramethyl-substituted diepoxy precursor, is presented. The transformation implies a thermal double deoxygenation followed by a stepwise double dehydrogenation reaction on the Au(111) surface, locally induced by inelastic tunneling electrons. This results in the transformation of *para*-dimethylbenzene moieties into non-aromatic *para*-quinodimethanes. The structures and electronic properties of the intermediate and final products are investigated at the single molecule level with high spatial resolution, using both scanning tunneling microscopy/spectroscopy and non-contact atomic force microscopy. The experimental results are supported by density functional theory calculations.

Introduction

Acenes are polycyclic aromatic hydrocarbons resulting from the linear *cata*-fusion of benzene rings, and are considered privileged compounds in the field of molecular materials.[1–4] However, their practical use is hampered by the decreased chemical stability associated to the extension of the length of the acene chain, a feature that can be well rationalized on the basis of Clar's π-sextet rule.[5] Given their highly reactive nature,[6] the synthesis of large acenes only by solution chemistry methods is problematic, and much remains to be understood about the electronic ground state of long acenes or the effect of introducing substituents or dopants. On-surface synthesis has been effective in the generation of higher acenes, also allowing to investigate their electronic properties in detail on a surface.[7–16] Very recently, the synthesis of the 13-ring acene, *i.e.* tridecacene, has been independently reported by two groups,[17,18] suggesting a nonmonotonous length-dependent HOMO-LUMO gap[17] and proving the predicted open-shell character[18] of extended acenes. Heteroatom substitution in long acenes has led the way to introducing *n*-type doping in their semi-conducting properties.[19–22] On the other hand, efforts have been devoted to the development of stable acene analogs through different strategies,[23] including the installation of suitable substituents in the periphery of the polycyclic system,[24] the generation of linear species with quinoidal conjugation,[25] or the introduction of structural elements which are able to break or partially interrupt the conjugation along the molecule, resulting in species with an increased number of Clar's sextets in the 1D framework. In this regard, the introduction of four-membered cyclobutadiene (CBD) rings has led to the solution-phase synthesis of stable CBD-containing oligoacenes[26–31] and to the on-surface construction of linear polycyclic structures containing nonbenzenoid moieties.[32–35] Less explored is the incorporation of fused six-membered 3,6-dimethylenecyclohexa-1,4-diene (*para*-quinodimethane, *p*-QDM) moieties in the acene backbone to disrupt conjugation, although successful examples of TCNQ-embedded long acenes (TCNQ = 7,7,8,8-tetracyanoquinodimethane) have been reported.[36]

In this work we propose the synthesis of an isomer of undecacene (**1**, $C_{46}H_{26}$), containing two four-membered rings and two *para*-quinodimethane moieties in its structure (Figure 1). Based on the number of Clar sextets (5 *vs.* 1, as shown in

[a] S. Sarkar, K. Ho Au-Yeung, F. Moresco
Center for Advancing Electronics Dresden, TU Dresden, 01062 Dresden, Germany
E-mail: francesca.moresco@tu-dresden.de
[b] B. Álvarez, D. Peña, D. Pérez
Centro de Investigación en Química Biolóxica e Materiais Moleculares (CiQUS) and Departamento de Química Orgánica, Universidade de Santiago de Compostela, 15782 Santiago de Compostela, Spain
E-mail: diego.pena@usc.es
dolores.perez@usc.es
[c] A. Cobas, D. Pérez
Departamento de Química Orgánica, Universidade de Santiago de Compostela, 15782 Santiago de Compostela, Spain
[d] R. Robles
Centro de Física de Materiales CFM/MPC (CSIC-UPV/EHU), 20018 Donostia-San Sebastián, Spain
[e] N. Lorente
Centro de Física de Materiales CFM/MPC (CSIC-UPV/EHU) and Donostia International Physics Center, 20018 Donostia-San Sebastián, Spain
[f] K. Ho Au-Yeung
Current address: Physikalisches Institut, Karlsruher Institut für Technologie, 76131 Karlsruhe, Germany

Supporting information for this article is available on the WWW under https://doi.org/10.1002/chem.202402297

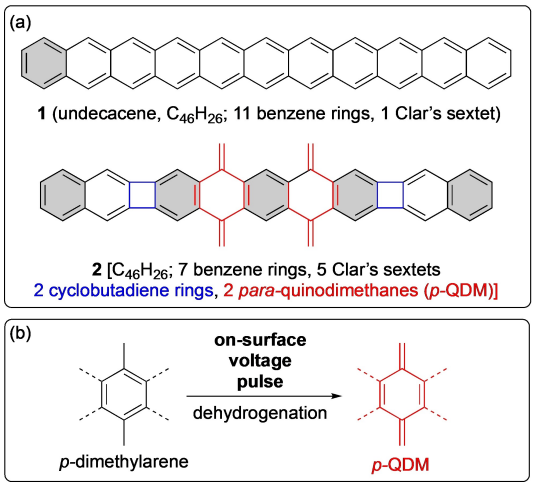

Figure 1. (a) Top: Structural features of undecacene **1**. Bottom: Structural features of undecacene isomer **2**. (b) Postulated generation of a *para*-quinodimethane (*p*–QDM) from a *para*-dimethylarene by means of on-surface dehydrogenation.

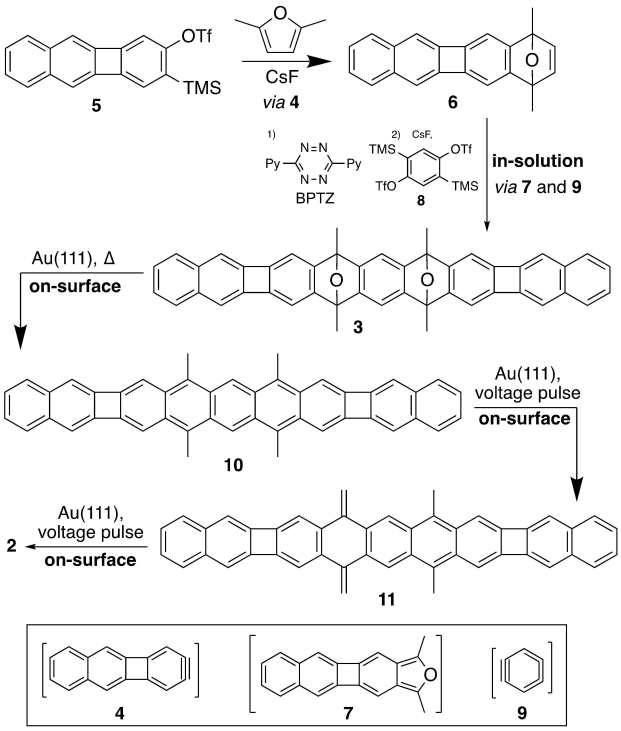

Scheme 1. Aryne-based synthesis of precursor 3 and its on-surface transformation into the novel undecacene isomer 2.

Figure 1a) and on the presence of nonbenzenoid rings, the target acene analog **2** is expected to show different electronic properties compared to undecacene. Particularly interesting is the introduction of *para*-quinodimethane (*p*-QDM) moieties, which have been scarcely explored in the field of on-surface synthesis. In principle the *p*-QDMs might be obtained by dehydrogenation of *para*-dimethylarenes (Figure 1b). However, it is worth noting that despite the early reports on the generation of the highly reactive, parent *p*-QDM (*p*-xylylene) by pyrolysis of *p*-xylene,[37] to the best of our knowledge, such a transformation has not been reported either in solution-phase chemistry or by on-surface synthesis.

Recently, several on-surface dehydrogenation reactions have been described, including those involving scanning tunneling microscopy (STM)-induced C–H bond cleavage at saturated carbon atoms, either for the generation of open-shell structures[38–42] or for the final aromatization of a partially saturated acene precursor.[14] Furthermore, tailor-made methyl-substituted aromatics have been exploited for the on-surface synthesis of graphene nanostructures with zigzag edges[43,44] or with five-membered rings[45] through processes involving thermally induced dehydrogenative intramolecular coupling reactions. Here, we present the synthesis of the undecacene isomer **2** on Au(111) starting from precursor **3** (Scheme 1), by a double deoxygenative aromatization followed by a stepwise double dehydrogenation reaction, involving a new on-surface reaction based on the transformation of *p*-dimethylarene moieties into non-linearly conjugated *p*-QDMs.

Results and Discussion

Based on previous successful results on the on-surface synthesis of acenes from epoxy derivatives,[9,16] compound **3** (Scheme 1) was devised as suitable precursor of the targeted compound **2**. Applying the aryne-based methodology for the construction of cyclobutadiene-containing oligoacenes recently described by some of us,[46] the synthesis of **3** was performed as shown in Scheme 1. Thus, the reaction of 2-benzo[*b*]biphenylyne **4**, generated from triflate **5**, with 2,5-dimethylfuran afforded adduct **6** in 89% yield. Treatment of **6** with 3,6-bis(pyridin-2-yl)-1,2,4,5-tetrazine (BPTZ) allowed the *in situ* generation of the isobenzofuranoid **7**, which was reacted with bistriflate **8** in the presence of CsF to give bisendoxide **3** in 20% yield, as the result of a formal double Diels-Alder reaction of diene **7** with 1,4-benzodiyne **9** (see SI for details and chemical characterization).

For the on-surface study, precursor **3** was deposited via flash/rapid evaporation from a silicon wafer onto a clean Au(111) surface kept at room temperature. This method allows the deposition in ultra-high vacuum (UHV) conditions of unstable or large molecules that would otherwise decompose before reaching their sublimation temperature.[16,47] Upon cooling the sample to 5 K, we observed in the STM images individual molecules, most of them with a linear shape and an apparent length of around 30 Å (see SI, Figure S3b). A STM image of a single molecule is shown in Figure 2a and an overview image in SI (Figure S3). We tentatively assigned it to compound **10**, containing a pentacene core, which would result from the deoxygenative aromatization of bisendoxide **3** (Scheme 1) happening during sublimation, a process that has been previously observed after flash evaporation of epoxyacenes on Au(111).[16] The bright protrusions at the center of the molecule can be attributed to the methyl groups. We also observed a few bent-shaped molecules (see SI, Figure S3),

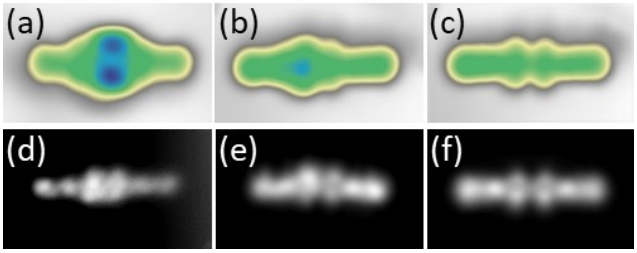

Figure 2. (a) – (c) Constant current STM images taken with a CO functionalized tip showing the step by step on-surface dehydrogenation of a single molecule via voltage pulses. Pulse parameters: 2.5 V, 1 nA, 5 seconds. Image parameters: V = −1 V, I = 100 pA. (d) – (f) Constant height STM images with CO functionalized tip taken after each pulse, showing all steps of the reaction. Image parameters: V = 10 mV. Image dimensions: 3.5 nm x 2.0 nm.

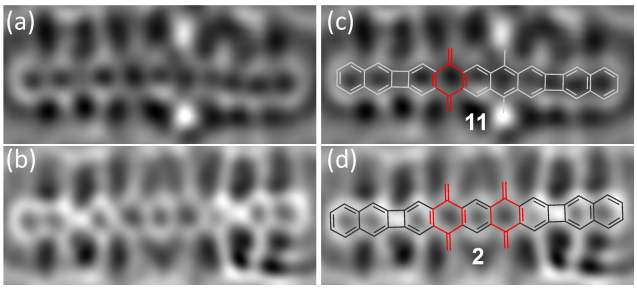

Figure 3. (a) Laplace filtered nc-AFM image with CO functionalized tip of the partially reacted species, assigned as **11**. (b) Laplace filtered nc-AFM image with CO functionalized tip of the final product, assigned as **2**. (c) Image 3a with the structure of **11** superimposed. (d) Image 3b with the structure of **2** superimposed. Scanning parameters: (a) Amplitude = 300 pm, V = 1 mV, size = 4.0 x 1.7 nm (b) Amplitude = 150 pm, V = 1 mV, size 4.0 nm x 1.7 nm.

which could result from the surface-mediated opening of one (or two) of the cyclobutadiene rings.[48] The assignment was confirmed by high-resolution non-contact atomic force microscopy (AFM) images, shown in Figure S3c.

Next, we focused on the linear molecules (Figure 2a) to further investigate the proposed on-surface dehydrogenation. After applying a voltage pulse with the STM tip (typically V = 2.5 V, I = 1 nA) the molecule of Figure 2a can be converted to a first product shown in Figure 2b, where the central bright protrusion appears split in two separated maxima with different intensities. A further voltage pulse causes the complete planarization of the molecule to obtain the symmetric species imaged in Figure 2c. This suggests that a stepwise process involving, in each step, the transformation of two peripheral C(sp^3)-hybridized methyl substituents into two C(sp^2)-hybridized methylidene groups has happened, that is, the sequential conversion of the *para*-dimethylarene moieties into *p*-QDMs. The pulsing sequence can be found in the SI (Figure S4).

We investigated in more detail the three observed molecular species by recording high resolution STM images in constant height mode using a CO functionalized tip (Figures 2d–f). The pronounced maximum around the central part observed in the STM images of the unpulsed molecule (Figure 2a) appears in the constant height CO-tip image (Figure 2d) formed by separated bright symmetric protrusions that we tentatively assign to the four methyl groups. After the first pulse, the intermediate product (Figures 2b,e) shows an asymmetry in the central lobes, *i.e.* one of the two lobes has a lower intensity after the pulse, suggesting the loss of two hydrogen atoms (one from each of two *para*-located methyl groups) while the other two remain unchanged. After the second pulse the molecule is symmetric and both lobes are flat (Figures 2c,f). We therefore tentatively assign the unpulsed molecule of Figures 2a,d to **10**, the intermediate species in Figures 2b,e to compound **11** and the final product (Figures 2c,f) to compound **2**.

We studied the intermediate and final products by bond-resolved non-contact AFM with a CO functionalized tip, as presented in Figure 3. The intermediate species appears asymmetric also in the AFM images (Figure 3a), showing a slight non-planarity and two local bright features indicating the two remaining methyl groups.[49] The symmetric final molecule, with well-resolved four-membered rings, is shown in Figure 3b. The pulse induced dehydrogenation is apparent when comparing Figures 3a,b, thus supporting the assignment of the intermediate to species **11** and of the final product to compound **2** (see Figures 3c,d).

Additionally, we investigated the proposed compounds **10**, **11** and **2** on the Au(111) surface by DFT calculations and image simulations. A preliminary computational study of the structures and properties of the molecules in the gas phase was also performed, including the analysis of the global and local aromaticity of the targeted oligoacene derivative **2** and of pentacene **10** by NICS-XY scan[50] and ACID plot[51,52] calculations (see SI section 7, Figures S10–S12 for details), showing the local nonaromatic character of the *p*-QDM rings in compound **2**.

The adsorption geometries of **10**, **11**, and **2** calculated by DFT on the Au(111) surface are shown in Figure 4a–c. The corresponding simulated STM images are presented in Figure 4d–f, showing a very good agreement with the experimental STM images of Figure 2, and therefore supporting the proposed reaction sequence and structure assignment. The enhanced surface interaction of the molecule with the *p*-QDM moieties as compared to the methylated species, as shown in

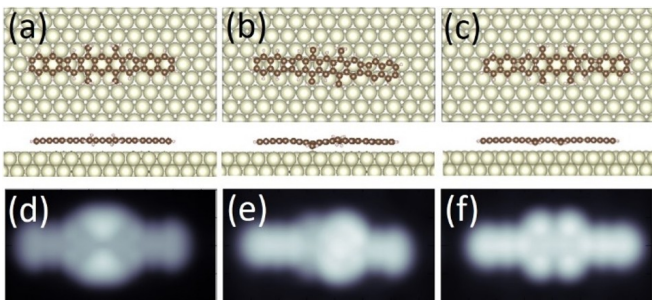

Figure 4. DFT calculations of molecular species on Au(111) (a) Top view and sideview of adsorption geometry of **10**. (b) Top view and sideview of adsorption geometry of **11**. (c) Top view and sideview of adsorption geometry of **2** and calculated STM topography. (d)–(f) Calculated STM images of **10**, **11** and **2**.

Figure 4b and Figure 4c, is also observed experimentally in the AFM images as a slight lowering of contrast (see Figure 3).

The electronic properties of the three species were investigated by scanning tunneling spectroscopy (STS) and density functional theory (DFT) simulations, as shown in Figure 5 for the final product that we assign to compound **2**. The STS spectrum, taken at the position marked in the inset STM topography image, is shown in Figure 5a. Below the Fermi energy, a broad and weak resonance peak starting at $V=-1.0$ V appears, while above the Fermi energy, a more intense broad resonance peak centered around $V=2$ V is observed.

The broadening of the peaks can be ascribed to the interaction of the molecule with the metal surface. To improve the energy resolution, and eventually observe the single resonances, it is possible to record constant current dI/dV maps at bias increments around the peak positions. By an increment of about 0.1 V, the highest contrast images are shown in the left column of Figure 5b while intermediate cases are reported in the SI (Figure S9). At negative bias, the highest contrast is observed at $V=(-1.05\pm0.10)$ V and shows a clear localization around the quinodimethanes, while weakly extending over the molecule.[16] Repeating this bias sweep on the positive side shows three distinct localizations. At $V=(1.84\pm0.10)$ V, the electronic contrast is restricted between the four–membered rings, with additional contrast around the central benzene ring. At $V=(2.04\pm0.10)$ V on the other hand, the contrast is localized around the neighboring benzenoid rings with diminished contribution from the central ring. Finally, at $V=(2.30\pm0.10)$ V the localization is centered strongly around the cyclobutadiene-fused benzenes. The experimental differential conductance maps are in very good agreement with the calculated ones presented in the right column of Figure 5b, confirming the assignment of the final reaction product and the contribution of the single orbitals to the observed resonances, with a HOMO-LUMO gap $E_g=2.9\pm0.10$ eV. Widening of the electronic gap of acene analogs due to the inclusion of cyclobutadiene units has been previously reported[32,34,46] and here we observe an even more pronounced effect as a result of the presence of the non-aromatic *p*-QDM moieties. Compared to undecacene, which has a gap $E_g=1.09$ eV,[15] our values are in the range of tetracene[7] ($E_g=2.9$ eV) due to the disruption of conjugation caused by the cyclobutadiene (partial) and *p*-QDM units.

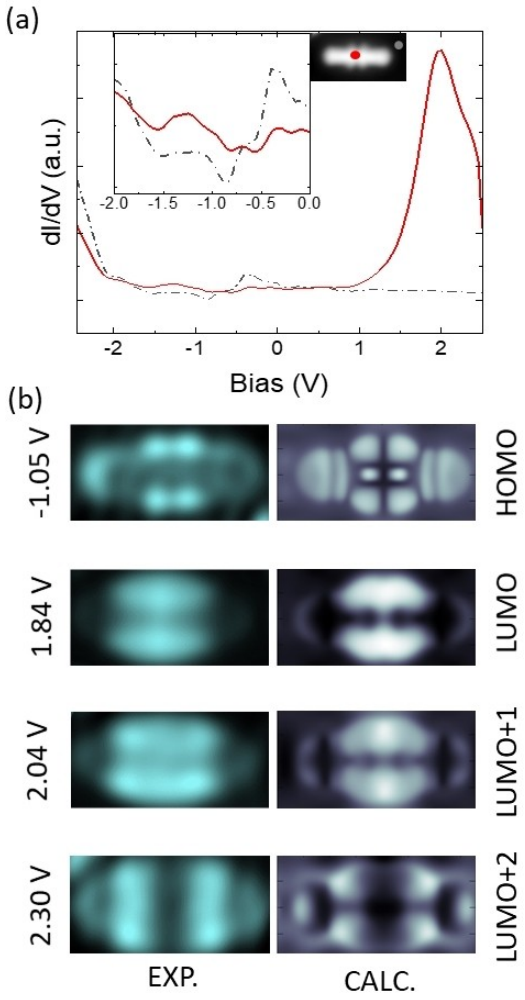

Figure 5. STS and constant current dI/dV maps: (a) STS of fully reacted molecule **2**; the spectrum was recorded at the position shown in the STM image of the inset. (b) dI/dV maps taken at specified bias values and corresponding calculated conductance maps. All images: 3.5 nm×1.7 nm.

We also studied by STS the electronic properties of the initial, unpulsed molecule, and of the intermediate product obtained after one voltage pulse. We found the experimental dI/dV maps in excellent agreement with the DFT simulations of the conductance maps for **10** and **11** (see SI, Figures S5, S6 and S7). These results indicate that the observed resonances are well described by the molecular orbitals of the adsorbed molecules and support the proposed structure of the initial compound as bis(naphthocyclobuta)-fused pentacene **10**, and the intermediate species as the single *p*-QDM-containing oligoacene **11**. The experimentally estimated energy gap for intermediate **11** is $Eg=2.7\pm0.10$ eV (see Figure S6). The slight opening of the bandgap of **2** in comparison with that of **11** is qualitatively expected due to the presence of an additional *p*-QDM moiety. However, DFT calculations show a large broadening and a strong hybridization of the electronic resonances on the gold surface, making a comparison of the HOMO-LUMO gap of intermediate and final products difficult.

Conclusions

In summary, our study delved into the synthesis of an isomer of undecacene featuring unconventional cyclobutadiene and *para*-quinodimethane structural motifs, by combining solution-phase and on-surface chemistry. Exploiting aryne cycloaddition reactions, we synthesized a diepoxyacene derivative that served as a precursor for fabricating the targeted undecacene isomer on the Au(111) surface. The key on-surface process involved the sequential generation of *para*-quinodimethane moieties from *para*-dimethylarenes via a controlled double dehydrogenation reaction triggered by voltage pulses. We thoroughly characterized the intermediate product resulting from a single dehydrogenation step. Accurate assignment of both intermediate and final products was facilitated by high-resolution scanning probe

microscopy and spectroscopy experiments, complemented by computational model simulations. Our findings provide a novel molecular transformation to the dynamic field of on-surface chemistry, while showcasing the potential to modulate the electronic properties of acenes through the incorporation of nonbenzenoid rings.

Experimental Section

General Synthetic Methods

All reactions were carried out under argon using oven-dried glassware. Anhydrous CH_2Cl_2 and CH_3CN were taken from a MBraun SPS-800 Solvent Purification System. Finely powdered CsF was dried under vacuum at 100 °C, cooled under argon and stored in a glove-box. 3-(Trimethylsilyl)benzo[b]biphenylen-2-yl triflate (**5**)[46] and bis(trimetilsilyl)phenynele-1,6-diyl bistriflate (**8**)[53] were prepared following previously described procedures, the latter being also commercially available from ABCR GmbH. Other commercial reagents were purchased from ABCR GmbH, Sigma-Aldrich or Fluorochem, and were used without further purification. TLC was performed on Merck silica gel 60 F254 and chromatograms were visualized with UV light (254 and 360 nm). Column chromatography was performed on Merck silica gel 60 (ASTM 230–400 mesh). ^{1}H and ^{13}C NMR spectra were recorded at 300 and 75 MHz, respectively, in a Varian Mercury-300 instrument. Atmospheric pressure chemical ionisation (APCI) HRMS were obtained on a Bruker Microtof, using either Flow Injection Analysis (FIA) for sample introduction. UV-Vis and fluorescence spectra were obtained on a Jasco V-630 and on a Fluoromax-2 spectrophotometers, respectively.

Synthesis of Compound 6

To a solution of **5**[46] (67 mg, 0.16 mmol) in dry CH_3CN (3.2 mL) placed in a Schlenk flask under argon, 1,5-dimethylfuran (230 mL, 3.17 μmol) and anhydrous CsF (218 mg, 1.40 mmol) were successively added. The reaction mixture was stirred at room temperature for 14 hours. The solvent was evaporated and the residue was suspended in CH_2Cl_2 and passed through a SiO_2 plug to isolate **6** as pale yellow solid (42 mg, 89%). ^{1}H NMR (300 MHz, $CDCl_3$), δ: 7.40 (dt, $J=7.1$, 3.5 Hz, 2H), 7.22 (dt, $J=5.9$, 3.5 Hz, 2H), 6.82(s, 2H), 6.77 (s, 2H), 6.74 (s, 2H), 1.88 (s, 6H). ^{13}C NMR-DEPT (75 MHz, $CDCl_3$), δ: 155.1 (C), 148.1 (C), 146.5 (CH), 146.3 (C), 135.2 (C), 128.5 (CH), 126.1 (CH), 113.7 (CH), 111.8 (CH), 88.8 (C), 15.4 (CH_3). HRMS(APCI-FIA-TOF) for $C_{22}H_{17}O$ ($[M+H]^+$) Calcd.: 297.1274; Found: 297.1271.

Synthesis of Compound 3

A solution of epoxyacene **6** (40 mg, 0.13 mmol) and 3,6-bis(pyridine-2-yl)-1,2,4,5-tetrazine (BPTZ) (35 mg, 0.15 mmol) in CH_2Cl_2 (4 mL) was stirred at 45 °C until complete consumption of the starting epoxyacene (TLC monitoring, 1.5 h), generating isobenzofuran **7** *in situ*. To this solution, kept at room temperature in a Schlenk flask, a solution of the 1,4-benzodiyne precursor **8** (35 mg, 0.07 mmol) in CH_3CN (4 mL) was added, followed by finely powdered, anhydrous CsF (123 mg, 0.81 mmol; addition of the solid under a positive flow of argon). The mixture was stirred at room temperature for 14 h, then the solvent was evaporated under reduced pressure and the desired bisendoxide was isolated by quick chromatography on NEt_3-deactivated silica gel (hexane/AcOEt; 9:1 to 3:2 gradient), to yield compound **3** as a yellow solid (8 mg, 20%). ^{1}H NMR (300 MHz, $CDCl_3$), δ: 7.32 (dd, $J=6.1$, 3.2 Hz, 4H), 7.15 (dd, $J=6.2$, 3.3 Hz, 4H), 6.98 (s, 2H), 6.76 (s, 4H), 6.67 (s, 4H), 2.02 (s, 12H). ^{13}C NMR-DEPT (75 MHz, $CDCl_3$), δ: 153.7(C), 150.1(C), 148.8(C), 146.1(C), 135.2(C), 128.5(CH), 126.2(CH), 114.0(CH), 111.7(CH), 110.4(CH), 87.1(C), 14.2(CH_3). HRMS(APCI-FIA-TOF) for $C_{46}H_{31}O_2$ ($[M+H]^+$) Calcd.: 615.2319; Found: 615.2316. UV-vis. ($CHCl_3$), λ_{max}: 272,302, 312, 320, 362, 381, 403 nm.

Experimental Methods for the On-Surface Study

The Au(111) crystal was cleaned by subsequent cycles of Ar^+ sputtering and annealing to 450 °C. STM experiments were performed using a custom-built instrument operating at a low temperature of $T=5$ K under ultra-high vacuum conditions ($p \approx 1\times10^{-10}$ mbar). The precursor molecules **3** were evaporated from an Si wafer that had been cleaned via direct heating. The Au(111) surface was kept at room temperature (25 °C) and following deposition, post-annealed to 200 °C. All STM images were recorded in constant-current mode, unless otherwise mentioned, with the bias voltage applied to the sample. All AFM experiments were conducted in the constant-height mode by using a q-Plus tuning fork (a resonance frequency $f_0 \approx 27$ kHz and a quality factor $Q >$ 47,000) with a CO terminated tip and images were obtained via frequency modulation.

To trigger the sequential reaction from **10** to **2**, the STM tip was positioned at a fixed height above a molecule (non-contact) with the feedback loop switched off and a voltage V was applied within a fixed time window. STM images were recorded both before and after each pulsing event.

All spectroscopy measurements were conducted in constant height mode, while dI/dV maps were obtained in constant current mode. Spectra and maps were measured using lock-in detection with a modulation frequency of 833 Hz and a modulation amplitude of 40 mV. Only those tips showing the Au(111) surface state were used for spectroscopy measurements on the molecules.

Computational Methods

Calculations in the gas phase were performed using the Gaussian 16 program package.[54] Geometries were optimized at the density functional level using the B3LYP functional[55] and 6–311 G(d) basis set. Vibrational frequency calculations were performed at this level to confirm the nature of the stationary points (minima, transition structures or saddle points) and to obtain the thermal and entropic contribution to the free energy. NICS-XY scans[50] were calculated with the Aroma package at the GIAO–B3LYP/6–311+G(d) computational level.[56,57] The NICS-*XY* scans contain only the π-contribution by employing the σ-only model.[58] The vertical excitation energies were calculated from the ground state geometries using time-dependent density functional theory (TDDFT) at the b3lyp/6–311++G(d,p) level of theory. To compute the anisotropy of the induced current density (ACID), the NMR shielding tensors were computed with the CSGT method at the same level of theory. The ACID plots were prepared with the ACID 3.0.4 software provided by the Herges' group.[51,52] The magnetic field vector was set perpendicular to the plane of the molecules. All surfaces are displayed with an isovalue of 0.04 a.u.

Model DFT calculations of the molecules adsorbed on Au(111) were performed with the VASP code,[59] using the PAW method[60] and the PBE exchange-correlation functional.[61] Missing long-range dispersion interactions in this functional were included following the Tkatchenko – Scheffler method.[62] A plane-wave basis set was used with an energy cutoff of 400 eV. The Au(111) surface was simulated by a four-layer slab and a $(13\times4\sqrt{3})$ surface unit cell. The coordinates of all atoms except the two bottom layers were optimized until forces were below 0.01 eV/Å. Geometry relaxations

were performed using the Gamma point, while STM images were simulated using a denser 2x4x1 k-grid mesh. STM images were computed using the Tersoff-Hamann approximation[63,64] as implemented in the STMpw code.[65]

Supporting Information Summary

Further experimental and computational details are given in the Supporting Information file.

Acknowledgements

This work was funded by the DFG Project 432345501, the European Innovation Council (EIC) under the project ESiM (grant agreement No 101046364), grants PD2019–110037GB–I00, PID2021–127917NB–I00, PID2022–139933NB–I00 and PID2022–140845OB–C62 funded by MICIU/AEI/ 10.13039/501100011033, QUAN-000021–01 funded by the Gipuzkoa Provincial Council and IT-1527–22 funded by the Basque Government the European Union Horizon 2020 through FET-Open Project SPRING (Grant No. 863098) and ERC Synergy Grant MolDAM (951519), the Xunta de Galicia (Centro singular de investigación de Galicia accreditation 2019–2022, ED431G 2019/03 and Oportunius Program) and the European Union (European Regional Development Fund-ERDF). Support from German Research Foundation (DFG) by the Collaborative Research Centre (CRC) 1415 is also gratefully acknowledged. We thank Alexander Tahn from the cfaed Dresden Center for Nanoanalysis (DCN), for FIB operations on the AFM tip and its SEM images. The authors thank the Centro de Supercomputación de Galicia (CESGA) for generous allocation of computer time.

Conflict of Interests

The authors declare no conflict of interest.

Data Availability Statement

The data that support the findings of this study are available in the supplementary material of this article.

Keywords: Acenes · Arynes · Aromaticity · On-surface synthesis · High-resolution AFM/STM

[1] J. E. Anthony, *Angew. Chem. Int. Ed.* **2008**, *47*, 452–483.
[2] Z. Sun, Q. Ye, C. Chi, J. Wu, *Chem. Soc. Rev.* **2012**, *41*, 7857–7889.
[3] M. Watanabe, K.-Y. Chen, Y. Chang, T. J. Chow, *Acc. Chem. Res.* **2013**, *46*, 1606–1615.
[4] C. Tönshoff, H. F. Bettinger, *Chem. Eur. J.* **2021**, *27*, 3193–3212.
[5] E. Clar, *The Aromatic Sextet*, John Wiley & Sons LTD, New York **1972**.
[6] P. V. R. Schleyer, M. Manoharan, H. Jiao, F. Stahl, *Org. Lett.* **2001**, *3*, 3643–3646.
[7] J. Krüger, N. Pavliček, J. M. Alonso, D. Pérez, E. Guitián, T. Lehmann, G. Cuniberti, A. Gourdon, G. Meyer, L. Gross, F. Moresco, D. Peña, *ACS Nano* **2016**, *10*, 4538–4542.
[8] J. Krüger, F. Eisenhut, J. M. Alonso, T. Lehmann, E. Guitián, D. Pérez, D. Skidin, F. Gamaleja, D. A. Ryndyk, C. Joachim, D. Peña, F. Moresco, G. Cuniberti, *Chem. Commun.* **2017**, *53*, 1583–1586.
[9] J. Krüger, F. García, F. Eisenhut, D. Skidin, J. M. Alonso, E. Guitián, D. Pérez, G. Cuniberti, F. Moresco, D. Peña, *Angew. Chem. Int. Ed.* **2017**, *56*, 11945–11948.
[10] J. Krüger, F. Eisenhut, D. Skidin, T. Lehmann, D. A. Ryndyk, G. Cuniberti, F. García, J. M. Alonso, E. Guitián, D. Pérez, D. Peña, G. Trinquier, J.-P. Malrieu, F. Moresco, C. Joachim, *ACS Nano* **2018**, *12*, 8506–8511.
[11] J. I. Urgel, H. Hayashi, M. Di Giovannantonio, C. A. Pignedoli, S. Mishra, O. Deniz, M. Yamashita, T. Dienel, P. Ruffieux, H. Yamada, R. Fasel, *J. Am. Chem. Soc.* **2017**, *139*, 11658–11661.
[12] J. I. Urgel, S. Mishra, H. Hayashi, J. Wilhelm, C. A. Pignedoli, M. Di Giovannantonio, R. Widmer, M. Yamashita, N. Hieda, P. Ruffieux, H. Yamada, R. Fasel, *Nat. Commun.* **2019**, *10*, 861.
[13] M. Zugermeier, M. Gruber, M. Schmid, B. P. Klein, L. Ruppenthal, P. Müller, R. Einholz, W. Hieringer, R. Berndt, H. F. Bettinger, J. M. Gottfried, *Nanoscale* **2017**, *9*, 12461–12469.
[14] R. Zuzak, R. Dorel, M. Krawiec, B. Such, M. Kolmer, M. Szymonski, A. M. Echavarren, S. Godlewski, *ACS Nano* **2017**, *11*, 9321–9329.
[15] R. Zuzak, R. Dorel, M. Kolmer, M. Szymonski, S. Godlewski, A. M. Echavarren, *Angew. Chem. Int. Ed.* **2018**, *57*, 10500–10505.
[16] F. Eisenhut, T. Kühne, F. García, S. Fernández, E. Guitián, D. Pérez, G. Trinquier, G. Cuniberti, C. Joachim, D. Peña, F. Moresco, *ACS Nano* **2020**, *14*, 1011–1017.
[17] Z. Ruan, J. Schramm, J. B. Bauer, T. Naumann, H. F. Bettinger, R. Tonner-Zech, J. M. Gottfried, *J. Am. Chem. Soc.* **2024**, *146*, 3700–3709.
[18] R. Zuzak, M. Kumar, O. Stoica, D. Soler-Polo, J. Brabec, K. Pernal, L. Veis, R. Blieck, A. M. Echavarren, P. Jelinek, S. Godlewski, *Angew. Chem. Int. Ed.* **2024**, *63*, e202317091.
[19] K. Eimre, J. I. Urgel, H. Hayashi, M. Di Giovannantonio, P. Ruffieux, S. Sato, S. Otomo, Y. S. Chan, N. Aratani, D. Passerone, O. Gröning, H. Yamada, R. Fasel, C. A. Pignedoli, *Nat. Commun.* **2022**, *13*, 511.
[20] M. Pinheiro, L. F. A. Ferrão, F. Bettanin, A. J. A. Aquino, F. B. C. Machado, H. Lischka, *Phys. Chem. Chem. Phys.* **2017**, *19*, 19225–19233.
[21] M. Stolar, T. Baumgartner, *Chem. Asian J.* **2014**, *9*, 1212–1225.
[22] W. Jiang, Y. Li, Z. Wang, *Chem. Soc. Rev.* **2013**, *42*, 6113–6127.
[23] M. Müller, L. Ahrens, V. Brosius, J. Freudenberg, U. H. F. Bunz, *J. Mater. Chem. C* **2019**, *7*, 14011–14034.
[24] W. Fudickar, T. Linker, *J. Am. Chem. Soc.* **2012**, *134*, 15071–15082.
[25] X. Shi, W. Kueh, B. Zheng, K.-W. Huang, C. Chi, *Angew. Chem. Int. Ed.* **2015**, *54*, 14412–14416.
[26] R. R. Parkhurst, T. M. Swager, *J. Am. Chem. Soc.* **2012**, *134*, 15351–15356.
[27] S. P. Luppino, T. M. Swager, *Synlett* **2016**, *28*, 323–326.
[28] Z. Jin, Y. C. Teo, N. G. Zulaybar, M. D. Smith, Y. Xia, *J. Am. Chem. Soc.* **2017**, *139*, 1806–1809.
[29] Z. Jin, Z.-F. Yao, K. P. Barker, J. Pei, Y. Xia, *Angew. Chem. Int. Ed.* **2019**, *58*, 2034–2039.
[30] E. G. Miller, M. Singh, S. Parkin, T. Sammakia, N. H. Damrauer, *J. Org. Chem.* **2023**, *88*, 12251–12256.
[31] J. Wang, M. Chu, J.-X. Fan, T.-K. Lau, A.-M. Ren, X. Lu, Q. Miao, *J. Am. Chem. Soc.* **2019**, *141*, 3589–3596.
[32] C. Sánchez-Sánchez, A. Nicolaï, F. Rossel, J. Cai, J. Liu, X. Feng, K. Müllen, P. Ruffieux, R. Fasel, V. Meunier, *J. Am. Chem. Soc.* **2017**, *139*, 17617–17623.
[33] C. Sánchez-Sánchez, T. Dienel, A. Nicolaï, N. Kharche, L. Liang, C. Daniels, V. Meunier, J. Liu, X. Feng, K. Müllen, J. R. Sánchez-Valencia, O. Gröning, P. Ruffieux, R. Fasel, *Chem. Eur. J.* **2019**, *25*, 12074–12082.
[34] I. Izydorczyk, O. Stoica, M. Krawiec, R. Blieck, R. Zuzak, M. Stępień, A. M. Echavarren, S. Godlewski, *Chem. Commun.* **2022**, *58*, 4063–4066.
[35] Y. Wang, W.-W. Gong, Y. Zhao, G.-Y. Xing, L.-X. Kang, F. Sha, Z.-Y. Huang, J.-W. Liu, Y.-J. Han, P. Li, D.-Y. Li, P.-N. Liu, *Angew. Chem. Int. Ed.* **2024**, *63*, e202318142.
[36] Q. Ye, J. Chang, K.-W. Huang, G. Dai, C. Chi, *Org. Biomol. Chem.* **2013**, *11*, 6285–6291.
[37] M. Szwarc, *Discuss. Faraday Soc.* **1947**, *2*, 46–49.
[38] S. Mishra, M. Vilas-Varela, L.-A. Lieske, R. Ortiz, S. Fatayer, I. Rončević, F. Albrecht, T. Frederiksen, D. Peña, L. Gross, *Nat. Chem.* **2024**, *16*, 755–761 https://doi.org/10.1038/s41557–023–01431–7.
[39] T. Wang, A. Berdonces-Layunta, N. Friedrich, M. Vilas-Varela, J. P. Calupitan, J. I. Pascual, D. Peña, D. Casanova, M. Corso, M. D. G. de Oteyza, *J. Am. Chem. Soc.* **2022**, *144*, 4522–4529.

[40] A. Zhao, Q. Li, L. Chen, H. Xiang, W. Wang, S. Pan, B. Wang, X. Xiao, J. Yang, J. G. Hou, Q. Zhu, *Science* **2005**, *309*, 1542–1544.
[41] K. Biswas, M. Urbani, A. Sánchez-Grande, D. Soler-Polo, K. Lauwaet, A. Matěj, P. Mutombo, L. Veis, J. Brabec, K. Pernal, J. M. Gallego, R. Miranda, D. Écija, P. Jelínek, T. Torres, J. I. Urgel, *J. Am. Chem. Soc.* **2022**, *144*, 12725–12731.
[42] S. Clair, D. G. de Oteyza, *Chem. Rev.* **2019**, *119*, 4717–4776.
[43] P. Ruffieux, S. Wang, B. Yang, C. Sánchez-Sánchez, J. Liu, T. Dienel, L. Talirz, P. Shinde, C. A. Pignedoli, D. Passerone, T. Dumslaff, X. Feng, K. Müllen, R. Fasel, *Nature* **2016**, *531*, 489–492.
[44] M. Vilas-Varela, F. Romero-Lara, A. Vegliante, J. P. Calupitan, A. Martínez, L. Meyer, U. Uriarte-Amiano, N. Friedrich, D. Wang, F. Schulz, N. E. Koval, M. E. Sandoval-Salinas, D. Casanova, M. Corso, E. Artacho, D. Peña, J. I. Pascual, *Angew. Chem. Int. Ed.* **2023**, *62*, e202307884.
[45] a) M. Di Giovannantonio, J. I. Urgel, U. Beser, A. V. Yakutovich, J. Wilhelm, C. A. Pignedoli, P. Ruffieux, A. Narita, K. Müllen, R. Fasel, *J. Am. Chem. Soc.* **2018**, *140*, 3532–3536; b) X. Xu, M. Di Giovannantonio, J. I. Urgel, C. A. Pignedoli, P. Ruffieux, K. Müllen, R. Fasel, A. Narita, *Nano Res* **2021**, *14*, 4754–4759.
[46] B. Álvarez, J. Janeiro, A. Cobas, M. A. Ortuño, D. Peña, E. Guitián, D. Pérez, *Adv. Synth. Catal.* **2024**, *366*, 961–969.
[47] B. Schuler, G. Meyer, D. Peña, O. C. Mullins, L. Gross, *J. Am. Chem. Soc.* **2015**, *137*, 9870–9876.
[48] J. P. Calupitan, T. Wang, A. Pérez Paz, B. Álvarez, A. Berdonces-Layunta, P. Angulo-Portugal, R. Castrillo-Bodero, F. Schiller, D. Peña, M. Corso, D. Pérez, D. G. de Oteyza, *J. Phys. Chem. Lett.* **2023**, *14*, 947–953.
[49] P. Chen, S. Fatayer, B. Schuler, J. N. Metz, L. Gross, N. Yao, Y. Zhang, *Energy Fuels* **2021**, *35*, 2224–2233.
[50] A. Stanger, *J. Org. Chem.* **2010**, *75*, 2281–2288.
[51] R. Herges, D. Geuenich, *J. Chem. Phys. A* **2001**, *105*, 3214–3220.
[52] D. Geuenich, K. Hess, F. Köhler, R. Herges, *Chem. Rev.* **2005**, *105*, 3758–3772.
[53] H. M. Duong, M. Bendikov, D. Steiger, Q. Zhang, G. Sonmez, J. Yamada, F. Wudl, *Org. Lett.* **2003**, *5*, 4433–4436.
[54] M. J. Frisch, G. W. Trucks, H. B. Schlegel, G. E. Scuseria, M. A. Robb, J. R. Cheeseman, G. Scalmani, V. Barone, G. A. Petersson, H. Nakatsuji, X. Li, M. Caricato, A. V. Marenich, J. Bloino, B. G. Janesko, R. Gomperts, B. Mennucci, H. P. Hratchian, J. V. Ortiz, A. F. Izmaylov, J. L. Sonnenberg, D. F. Williams, F. Lipparini, F. Egidi, J. Goings, B. Peng, A. Petrone, T. Henderson, D. Ranasinghe, V. G. Zakrzewski, J. Gao, J. Rega, N. Zheng, G. Liang, W. Hada, M. Ehara, M. Toyota, K. Fukuda, R. Hasegawa, M. Ishida, T. Nakajima, Y. Honda, O. Kitao, H. Nakai, T. Vreven, K. Throssell, J. A. Montgomery Jr., J. E. Peralta, F. Ogliaro, M. J. Bearpark, J. J. Heyd, E. N. Brothers, K. N. Kudin, V. N. Staroverov, T. A. Keith, R. Kobayashi, J. Normand, K. Raghavachari, A. P. Rendell, J. C. Burant, S. S. Iyengar, J. Tomasi, M. Cossi, J. M. Millam, M. Klene, C. Adamo, R. Cammi, J. W. Ochterski, R. L. Martin, K. Morokuma, O. Farkas, J. B. Foresman, D. J. Fox, Gaussian 16 Rev. C.01, Wallingford, CT, **2016**.
[55] A. D. Becke, *J. Chem. Phys.* **1993**, *98*, 5648–5652.
[56] R. Gershoni-Poranne, A. Stanger, *Chem. Eur. J.* **2014**, *20*, 5673–5688.
[57] K. Woliński, A. J. Sadlej, *Mol. Phys.* **1980**, *41*, 1419–1430.
[58] K. Wolinski, J. F. Hinton, P. Pulay, *J. Am. Chem. Soc.* **1990**, *112*, 8251–8260.
[59] G. Kresse, J. Furthmüller, *Phys. Rev. B* **1996**, *54*, 11169–11186.
[60] G. Kresse, D. Joubert, *Phys. Rev. B* **1999**, *59*, 1758–1775.
[61] J. P. Perdew, K. Burke, Y. Wang, *Phys. Rev. B* **1996**, *54*, 16533–16539.
[62] A. Tkatchenko, M. Scheffler, *Phys. Rev. Lett.* **2009**, *102*, 073005.
[63] J. Tersoff, D. R. Hamann, *Phys. Rev. B* **1985**, *31*, 805–813.
[64] M.-L. Bocquet, H. Lesnard, S. Monturet, N. Lorente, in *Computational Methods in Catalysis and Materials Science: An Introduction for Scientists and Engineers* (Eds.: R. A. van Santen, P. Sautet), Wiley-VCH Verlag GmbH & Co., **2009**, pp. 199–219.
[65] N. Lorente, R. Robles, STMpw (Zenodo) DOI: 10.5281/zenodo.3581159 (accessed December 17, 2019).

Manuscript received: July 6, 2024
Accepted manuscript online: July 20, 2024
Version of record online: September 16, 2024